

EXPERIMENTAL INVESTIGATION OF THE FLOW-INDUCED VIBRATION OF A CURVED CIRCULAR CYLINDER

Gustavo R.S. Assi*

University of São Paulo, Brazil
Dept. Naval Arch. & Ocean Eng. – NDF Group

Cesar M. Freire

University of São Paulo, Brazil
Dept. Mechanical Eng. – NDF Group

Ivan Korkischko

University of São Paulo, Brazil
Dept. Mechanical Eng. – NDF Group

Narakorn Srinil

University of Strathclyde, Glasgow, UK
Dept. Naval Arch. & Marine Eng.

ABSTRACT

Experiments have been conducted in a water channel in order to investigate the vortex-induced vibration (VIV) response of a rigid section of a curved circular cylinder. Two curved configurations were tested regarding the direction of the approaching flow, a concave or a convex cylinder, in addition to a straight cylinder that served as reference.

Amplitude and frequency response are presented versus reduced velocity for a wide Reynolds number range between 750 and 15,000. Results showed that the curved cylinders presented significant less vibration for both concave and convex configurations when compared to the typical VIV response of a straight cylinder.

The concave configuration presented relatively high amplitudes of vibration that are sustained beyond the typical synchronisation region. We believe this distinct behaviour between the convex and the concave configurations is related to the wake interference happening in the lower half of the curvature due to perturbations generated in the horizontal section when it is positioned upstream.

Particle-image velocimetry (PIV) measurements of the separated flow along the cylinder highlight the effect of curvature on vortex formation and excitation revealing an interesting and complex fluid-structure interaction mechanism.

*Corresponding author: g.assi@usp.br. Address: PNV Dept. Eng. Naval e Oceânica, Escola Politécnica da Universidade de São Paulo, Av. Prof Mello Moraes 2231, 05508-030, São Paulo - SP, Brazil. www.ndf.poli.usp.br.

NOMENCLATURE

D	Cylinder external diameter
h	Cylinder vertical length below the water line
m^*	Mass ratio
ζ	Structural damping ratio
f_0	Cross-flow natural frequency in air
U	Flow speed
U/Df_0	Reduced velocity
\hat{x}	Streamwise harmonic amplitude of vibration
\hat{y}	Cross-flow harmonic amplitude of vibration
f_x	Streamwise oscillating frequency
f_y	Cross-flow oscillating frequency
Re	Reynolds number
St	Strouhal number

INTRODUCTION

Ongoing deep-sea explorations, installations and productions of hydrocarbon energy need the development of new viable technologies. One of these is the requirement of a robust and completely-reliable analysis tool for the prediction of vortex-induced vibration (VIV) of marine structures exposed to ocean currents. Because VIV can cause high cyclic-loading fatigue damage of structures, it is now widely accepted that VIV is a crucial factor that should be taken into account in the preliminary analysis and design. However, many insightful VIV aspects are still unknown and far from fully understood; these render the structural design quite conservative with the use of a large factor of safety. For offshore structures with initial curvatures and high flexibility such as catenary risers,

mooring cables and free-spanning pipelines, the theoretical, numerical or experimental VIV research is still very lacking.

Risers are very long pipes used to carry oil from the sea bed to offshore platforms floating on the water surface. Under the effect of sea currents, these flexible structures are especially susceptible to flow-induced vibrations, particularly since they have a relatively low mass compared to the mass of the displaced fluid. Generally, an offshore floating platform accommodates more than 40 riser pipes together with many other cylindrical structures. The interaction of these flexible structures can produce an even more complex problem, resulting in vibrations with rather unexpectedly higher amplitudes [1]. Flow interference from the platform hull, the soil on sea bed and the pipe itself can also increase the complexity of the flow, generating complex responses.

The riser may respond with different amplitudes and frequencies depending on the flow excitation and structural stiffness along the length of the pipe. Consequently, several modes of vibration with varying curvature appear along the span resulting in a very rich fluid-structure interaction mechanism [2]. In addition to that, flexible risers can be laid out in a catenary configuration which results in high curvature close to the region where it touches the bottom of the ocean, called the touchdown point.

In an attempt to understand and model the fluid-dynamic behaviour around curved sections of risers we have performed experiments with a curved section of rigid cylinder in a water channel. This idealised experiment is far from reproducing the real conditions encountered in the ocean, nevertheless it should throw some light on understanding how the vortex shedding mechanism is affected by the curvature of the pipe.

An investigation into the vortex shedding patterns and the fundamental wake topology of the flow past a stationary curved circular cylinder has been carried out by Miliou et al. [3] based on the computational fluid dynamics studies. As a result of pipe initial curvatures, the flow visualizations highlight different kinds of wake characteristics depending on the pipe (convex or concave) configuration and its orientation with respect to (aligned with or normal to) the incoming flow. When the flow is uniform and normal to the curvature plane, the cross-flow wake dynamics of curved pipes behave qualitatively similar to those of straight pipes. This is in contrast to the case of flow being aligned with the curvature plane where wake dynamics change dramatically. However, these scenarios are pertinent to a particular stationary cylinder case in a very low-Reynolds number range. The VIV behaviours will further transform if the structure oscillates and in-

teracts with the fluid wakes, depending on several fluid-structure parameters.

EXPERIMENTAL ARRANGEMENT

Experiments have been carried out in the Circulating Water Channel of the NDF (Fluids and Dynamics Research Group) at the University of São Paulo, Brazil. The NDF-USP water channel has an open test section 0.7m wide, 0.9m deep and 7.5m long. Good quality flow can be achieved up to 1.0m/s with turbulence intensity less than 3%. This laboratory has been especially designed for experiments in flow-induced vibrations and more details about the facilities are described in Assi et al. [4].

A rigid section of a curved circular cylinder, with an external diameter of $D = 32\text{mm}$, was made of ABS plastic and Perspex tubes according to the dimensions shown in Figure 1. The curved cylinder was composed of a horizontal section with $10D$ in length, a curved section with a $10D$ radius and a vertical section with length h/D that could be varied with reference to the water line. The water level was set to 700mm from the floor of the channel, which means that the $10D$ -long horizontal part of the cylinder was not close enough to the floor to suffer interference from the wall.

The model was connected by its upper end to a long pendulum rig (length $H = 3.0\text{m}$) that allowed the system to oscillate in two degrees of freedom (2dof) in the cross-flow and streamwise directions. The model was attached to two pairs of coil springs that provided the stiffness of the system. The springs were set to provide the same natural frequency (f_0) in both the cross-flow and streamwise directions. The design and construction of the pendular elastic rig was made by Freire et al. [5] based on a previous idea employed by Assi et al. [6, 7] for experiments with VIV suppressors. The present apparatus has been validated for VIV experiments by Freire et al. [8, 9].

Two laser sensors measured the cross-flow and streamwise displacements of the pendulum referring to the displacement of the bottom tip of the models. An especially built load cell was installed between the cylinder and the pendulum arm to allow for instantaneous measurements of lift, drag and torque acting on the cylinder. (Hydrodynamic forces will not be discussed in this paper.) A particle-image velocimetry (PIV) system was employed to analyse the wake along the span.

Regarding the flow direction, two orientations were investigated: a convex and a concave configuration according to the direction of the flow approaching the curvature. The flow direction in the test section of the water channel was not changed; naturally the curved cylinder

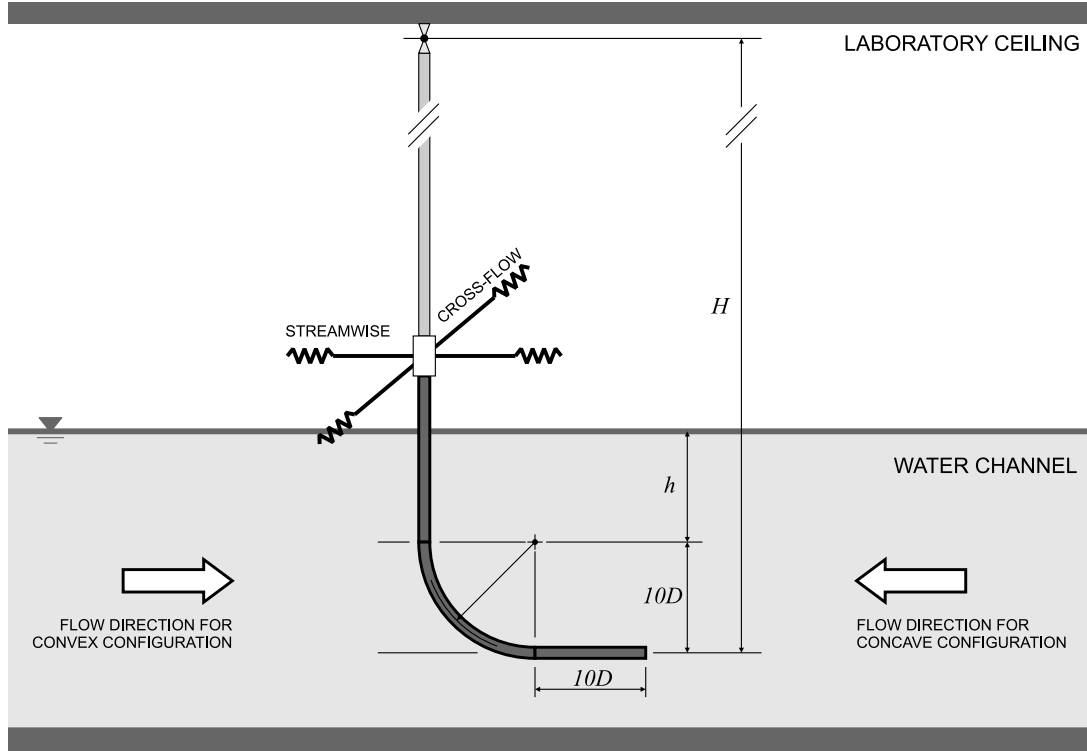


FIGURE 1: Experimental arrangement in the NDF-USP circulating water channel. The flow direction could not be changed in the water channel; in practice, the cylinder was rotated to arrange concave and convex configurations.

TABLE 1: Structural properties.

	m^*	ζ	$m^*\zeta$
Straight cylinder	2.8	0.2%	0.0056
Curved cylinders	2.1	0.2%	0.0042

was rotated to allow for both concave and convex arrangements. This is also illustrated in Figure 1.

Decay tests have been performed in air in order to determine the natural frequencies of the system in both directions as well as the level of structural damping. The apparatus with one universal joint and four springs turned out to present a very low structural damping of $\zeta = 0.2\%$, measured as a fraction of the critical damping. The total oscillating mass of the system was measured in air, resulting in a non-dimensional mass ratio m^* , defined as the ratio between the total mass and the mass of displaced fluid. Consequently, the mass-damping parameter $m^*\zeta$ of the system was kept to the lowest possible value in order to amplify the amplitude of response.

Table 1 presents a summary of the structural parameter for both the straight and curved cylinder.

RESULTS OF A STRAIGHT CYLINDER

A preliminary VIV experiment was performed with a straight cylinder in order to validate the set-up and methodology. The same pendulum rig was employed, only replacing the curved model by a straight cylinder with the same diameter. This time, the straight cylinder was long enough to reach the bottom wall only leaving a 3mm clearance to allow for free movement of the pendulum in any direction.

The dynamic response of the straight cylinder covered a reduced velocity range from 1.5 to 12, where reduced velocity (U/Df_0) is defined using the cylinder natural frequency of oscillation measured in air. The only flow variable changed during the course of the experiments was the flow velocity U , which, as for full-scale risers, alters both the reduced velocity and the Reynolds number between 750 and 15,000 for a maximum reduced velocity of 20.

Throughout the study, cylinder displacement amplitudes (\hat{x}/D for the streamwise and \hat{y}/D for the cross-flow directions) were found by measuring the root mean square value of response and multiplying by the square root of 2 (the so called harmonic amplitude). This is likely to give an underestimation of maximum response but was judged to be perfectly acceptable for assessing the general be-

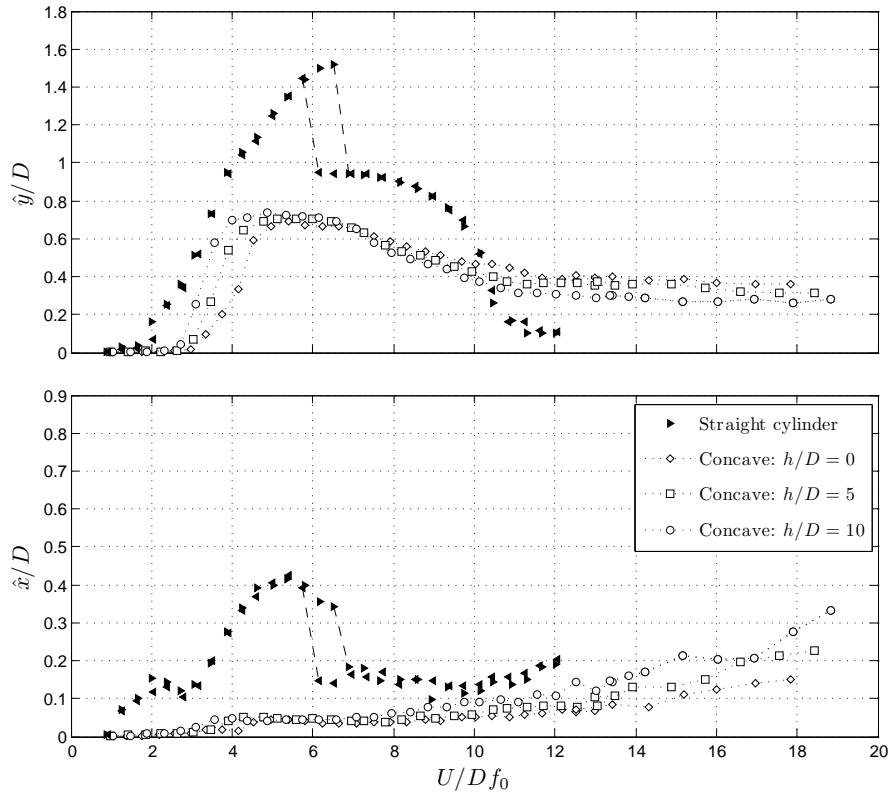


FIGURE 2: Cross-flow (\hat{y}/D) and streamwise (\hat{x}/D) amplitude of vibration versus reduced velocity for a straight cylinder and concave configurations varying the vertical section length (h/D).

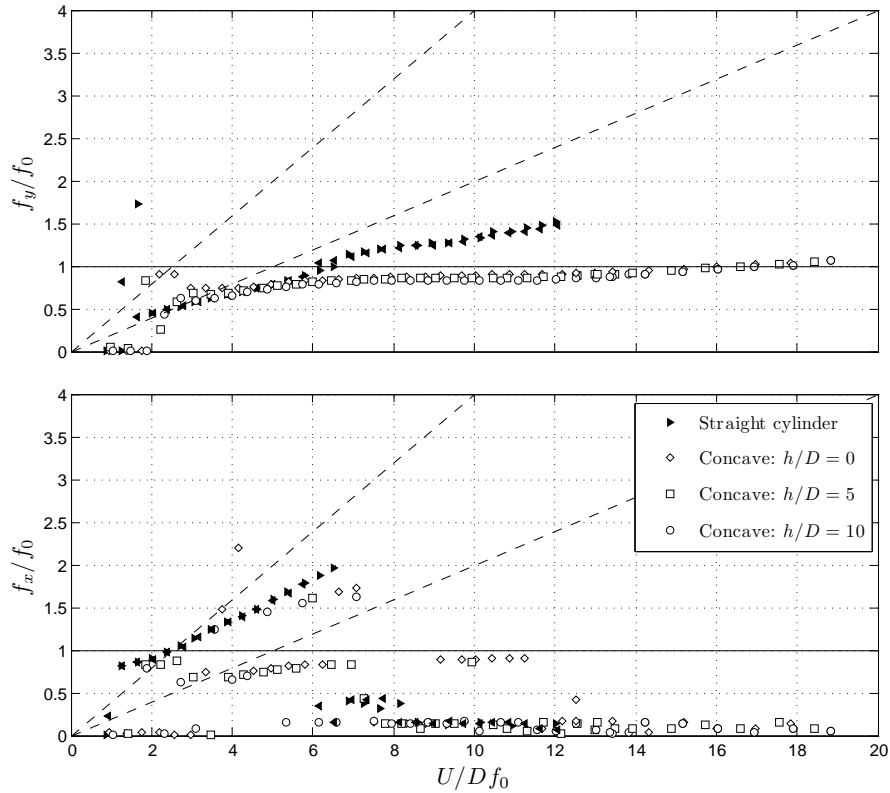


FIGURE 3: Cross-flow (\hat{y}/D) and streamwise (\hat{x}/D) dominant frequency of response versus reduced velocity for a straight cylinder and curved concave configurations varying the vertical section length (h/D).

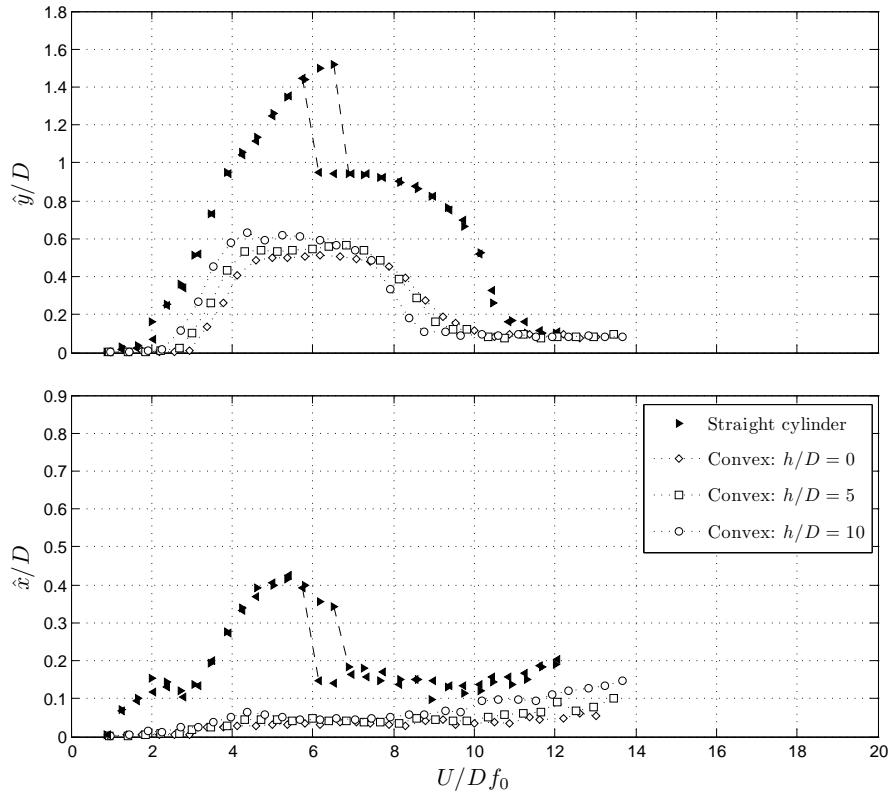


FIGURE 4: Cross-flow (\hat{y}/D) and streamwise (\hat{x}/D) amplitude of vibration versus reduced velocity for a straight cylinder and convex configurations varying the vertical section length (h/D).

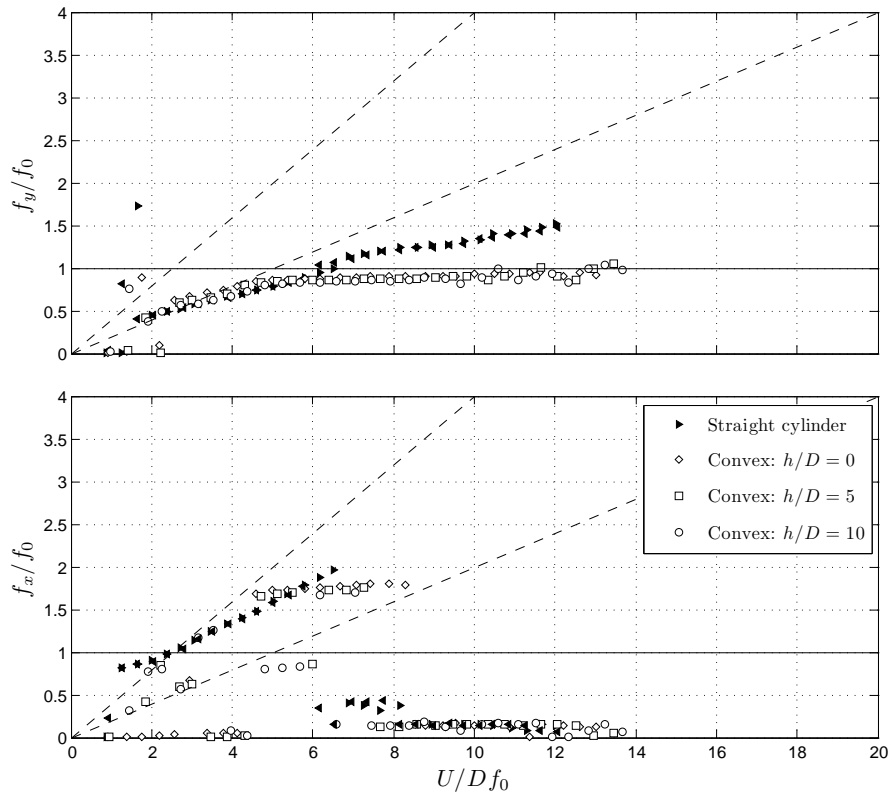


FIGURE 5: Cross-flow (\hat{y}/D) and streamwise (\hat{x}/D) dominant frequency of response versus reduced velocity for a straight cylinder and curved convex configurations varying the vertical section length (h/D).

haviour of VIV, since the response is mostly harmonic. Results presented in the present study correspond to the displacement of the lowest point of the model, i.e., the end of the cylinder closer to the section floor, thus representing the maximum displacement developed by each model. Displacements are non-dimensionalised by the cylinder diameter D .

Figures 2 and 4 compare the reference cross-flow and streamwise responses obtained from two different runs with the straight cylinder. In the first one, flow speed was increased in 30 steps from zero to a maximum, while in the second it was decreased from the maximum to zero. Both data sets overlap rather well for all the reduced velocity range except for a region around $U/Df_0 = 6$ where the well-known phenomenon of hysteresis in the VIV response has been observed. The streamwise VIV response also seems to occur in two resonance ranges ($U/Df_0 = 2$ and 6), the so-called second and third instability ranges involving asymmetric vortices.

Although the observed peak amplitude of $\hat{y}/D = 1.5$ around $U/Df_0 = 6$ is slightly higher than other results found in the literature for similar values of m^* (for example, Assi et al. [6]) the general behaviour of both curves show a typical response for 2-dof VIV. The higher amplitude found here could be explained by the very low mass-damping characteristics of the system and the geometric projection of the amplitude at the tip of the model and not at mid-length as usual.

Although the cylinder was initially aligned in the vertical position, in flowing water the mean drag displaces the cylinder from its original location reaching a slightly inclined configuration from the vertical. This was judged not to be detrimental to the experiment; hence the inclination of the cylinder was not corrected between each step. The same procedure was adopted for the curved cylinder.

Figures 3 and 5 present the dominant frequency of response versus reduced velocity. The dataset for the straight cylinder is repeated in both figures to serve as reference. Two dashed lines inclined with different slopes represent the region for a Strouhal number of 0.2 and 0.4, i.e., an estimation of the vortex shedding frequency for a straight cylinder in the cross-flow and streamwise direction respectively. It is clear that the straight cylinder presents a typical VIV response oscillating in the cross-flow direction with a frequency following the $St = 0.2$ line up to the beginning of the upper branch. Eventually, f_y/f_0 departs from $St = 0.2$ towards the unity value. The behaviour observed for the streamwise vibration is also typical of VIV with the difference that the frequency of response is twice as that for the cross-flow direction during much of the synchronisation range.

RESPONSE OF THE CURVED CYLINDERS

As mentioned above, experiments with the curved cylinder were performed taking into account two distinct configurations as far as the flow direction is concerned. In the concave configuration the flow approaches the model reaching first the horizontal section. As opposed to that, in the convex configuration the horizontal section is placed downstream of the curved and vertical parts.

Amplitude of vibration

In general terms, as presented in Figures 2 and 4, the curved cylinders showed significantly less vibration for both concave and convex configurations when compared to the typical VIV response of the straight cylinder. Such a reduction is noticeable in both the cross-flow and streamwise responses. This clearly shows that the curvature of the cylinder modifies the vortex shedding mechanism in a manner that the structure extracts less energy from the flow. We shall return to this point when investigating the velocity flow field with PIV.

For each concave and convex configuration, the vertical section of the cylinder close to the free surface was varied in three different lengths: $h/D = 0, 5$ and 10. The overall response for the three values of h/D is very similar, showing only minor differences at the beginning of the synchronisation range between $U/Df_0 = 3.0$ and 5.0. Apart from that, no distinct behaviour was observed as far as a variation in h/D is concerned for both concave and convex configurations.

The cross-flow displacement does not reveal distinct upper and lower branches of vibration such as those observed for a straight cylinder, but it produces a smooth curve that spans the whole synchronisation region with maximum amplitude around $\hat{y}/D = 0.75$ for the concave and 0.65 for the convex configurations. No hysteresis is found.

However, the most interesting feature of such a behaviour is found when the convex response is compared with the concave one (Figures 2 and 4). While the convex curve for \hat{y}/D drops immediately between $U/Df_0 = 8$ and 10 to a level of $\hat{y}/D \approx 0.1$, the response for the concave case does not diminish, but is sustained for higher reduced velocities around $\hat{y}/D = 0.3$ until the end of the experiment. Apparently there must be a fluidelastic mechanism occurring for reduced velocities above 8.0 for the concave configuration capable of extracting energy from the flow to sustain vibrations around $\hat{y}/D = 0.3$. We shall discuss this point later while analysing the PIV flow fields.

In the streamwise direction the responses of the curved cylinders are different from the typical VIV de-

veloped by the straight cylinder. Streamwise vibrations in the first and second resonance regions are totally suppressed, probably owing to the hydrodynamic damping effect induced by the cylinder's horizontal part. At the same time, the streamwise vibration \hat{x}/D for the concave case also shows increasing amplitude taking off for reduced velocities higher than 10 and reaching $\hat{x}/D \approx 0.35$ for the highest flow speed. It coincides with the increased amplitude observed in the cross-flow direction and should be related to the same excitation mechanism. Once more, no distinct difference in the streamwise response was observed while varying h/D .

Frequency of vibration

Figures 3 and 5 present the dominant frequency of oscillation non-dimensionalised by the natural frequency for both cross-flow and streamwise directions of motion. Apart from a few data points at very low reduced velocities (small amplitudes result in broader spectrum analysis), the cross-flow frequency of oscillation for the straight cylinder follows the expected behaviour along the $St = 0.2$ line, departing from it towards unity for reduced velocities beyond the resonance peak. The streamwise dominant frequency is also in agreement with other results in the literature and follows the line with double the Strouhal frequency for the equivalent of the initial and upper branches of cross-flow vibration.

Results for the curved cylinder show a consistent behaviour in the cross-flow direction, with data points following the Strouhal line up to the upper branch peak but remaining closer to $f_y/f_0 = 1.0$ for the rest of the reduced velocity range. In the streamwise direction, we find data points following both Strouhal lines and also very low frequencies indicating random drifts instead of periodic oscillations. Since the displacements in the streamwise direction are much smaller for the curved cylinder than the straight one, we should expect broader frequency spectra dominating over the response.

One might remember that the straight and curved cylinder should have very similar values of added mass in the cross-flow direction, but slightly different values in the streamwise direction due to the geometric properties relative to the flow. We have not taken such effect into account in this paper, but it might be playing an important role defining the frequencies of oscillation in water.

Trajectories of motion

Figure 6 qualitatively compares samples of displacement trajectories obtained for three experiments performed with the straight cylinder and the curved cylin-

ders with $h/D = 10$. The straight cylinder presents distinct eight-shape figures typical of 2dof VIV owing to the 2:1 ratio on the streamwise to cross-flow frequency of excitation. On the other hand, trajectories for both configurations of the curved cylinder reveal that the streamwise displacement is greatly reduced when compared to the straight cylinder. Both concave and convex cases show very little movement in the streamwise direction for the whole range of reduced velocity.

Another interesting observation relates the movement of both curved cylinders. It is clear that for reduced velocities greater than 10 the convex cylinder shows little displacement in both direction, while vibrations are sustained until the end of the experiment for the concave case as shown in Figures 2 and 4.

VELOCITY FIELDS

PIV measurements of the flow around the cylinder were performed for both concave and convex configurations as presented in Figures 7 to 10. Four visualisation areas for each configuration, labelled A1 to A4, were conveniently distributed along the length of the cylinder in order to evaluate as much as possible to flow pattern around the body. All four areas are in the same plane illuminated by the laser, which is parallel to the plane of curvature only dislocated by $1D$ from the centre of the cylinder in order to capture the highest velocities induced by the vortex tubes. Figures 8 and 10 show the location of each area composing the flow field along the cylinder. It is important to note that each velocity field was obtained from a different acquisition; hence A1, A2, A3 and A4 are not correlated in time.

All PIV measurements were performed for a static cylinder at $Re \approx 1000$. Of course the wake pattern for the static cylinder is expected to be different from the wake of an oscillating cylinder, but such an analysis of a fixed body can contribute to the understanding of the complex vortex-structure interaction occurring during the response. A similar approach was employed by Miliou et al. [3] who performed numerical simulations for a static, curved cylinder around $Re = 100$ to 500.

With that in mind, let us analyse first the flow pattern around the concave configuration in Figures 7 and 8. The overall flow around the body can be divided in two parts:

(I) Areas A1 and A2 show the region where the flow is mostly parallel to the axis of the cylinder. Therefore, no clear vortex tubes are observed with concentrated axial vorticity. Instead, the flow along the horizontal length is disturbed by the separation occurring at the tip of the cylinder. Area A1 shows the flow approaching the disk

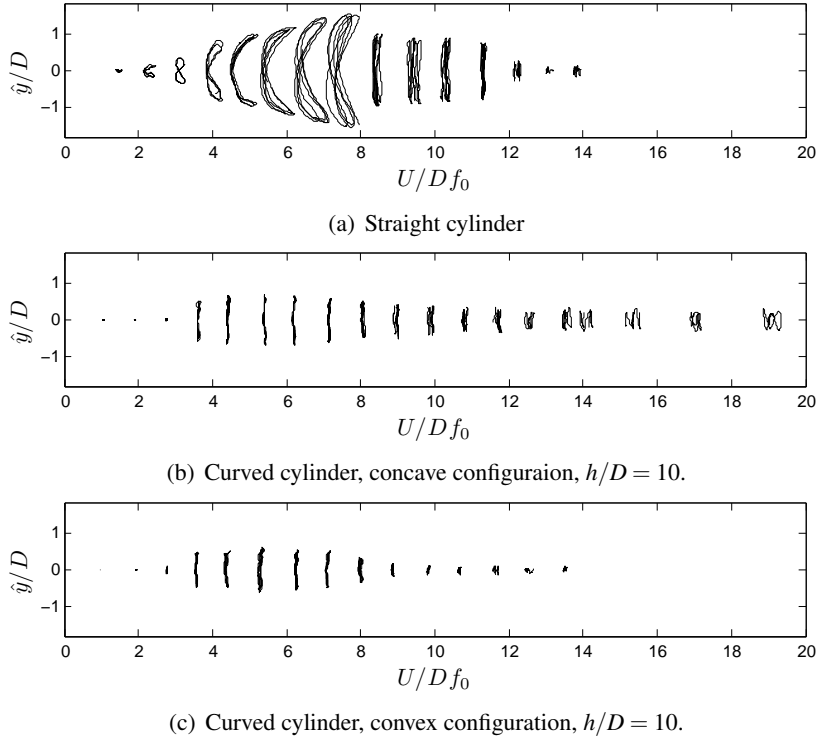


FIGURE 6: Response trajectories of motion for a (a) straight cylinder and a curved cylinder in (b) concave and (c) convex configurations.

facing upstream and separating into a recirculation bubble. The periodicity of the shedding associated with this region is also related to the flow speed and the diameter D , but no coherent vortices parallel to the cylinder is able to form. As a consequence, a cascade of small vortices is convected downstream along the horizontal length (see area A2) reaching the beginning of the curved section.

(II) Areas A3 and A4 show the region where the flow is mainly perpendicular to the axis of the cylinder. Coherent vortex tubes tend to form following the curvature of the body, but further downstream they are stretched and rapidly breakdown into smaller vortices that are convected by the flow. Area A3 show the instant when a vortex tube is shed almost tangent to the curvature, while area A4, around the vertical section, reveal a formation region more or less aligned with the axis of the cylinder. Streamlines drawn in areas A3 and A4 reveal a non-negligible velocity component deflecting the flow downwards immediately after the vortex formation region. As we move along the cylinder towards the water line from A3 to A4 the downward component is gradually reduced until it eventually disappears towards the upper half of A4. This region marks the competition between two wake modes existent along the transition from curved to straight cylinder. This looks similar to Fig. 15 in Miliou et al. [3], with $Re = 100$, although without the cylinder horizontal sec-

tion therein.

Analysing the flow pattern for the convex configuration in Figures 9 and 10 we notice two striking differences:

(I) Because the flow approaching the convex body does not encounter a blunt disk facing upstream, no strong separation or recirculation bubble is formed. As a consequence, the horizontal section seen in areas A1 and A2 is not exposed to a disturbed, unsteady flow parallel to the axis of the cylinder. In fact, A1 and A2 reveal that the upper half of the horizontal length is exposed to a periodic flow formed by a regular wake, while the bottom half experiences almost no perturbation, with streamlines showing a well behaved flow field parallel to the axis.

(II) Now, looking at the upper half of the body (A3 and A4) we notice much stronger and coherent vortex tubes when compared to the flow around the concave configuration. Area A3 reveals some kind of vortex dislocation after a formation region that increases in length as we move upwards. Because the convex geometry does not encourage the vortex tubes to stretch and break, a periodic wake seems to be sustained farther downstream. In contrast with the flow around the concave configuration, the velocity field around the curved section has a non-negligible vertical component upwards. It is stronger in A2 and is gradually reduced as we move upwards along

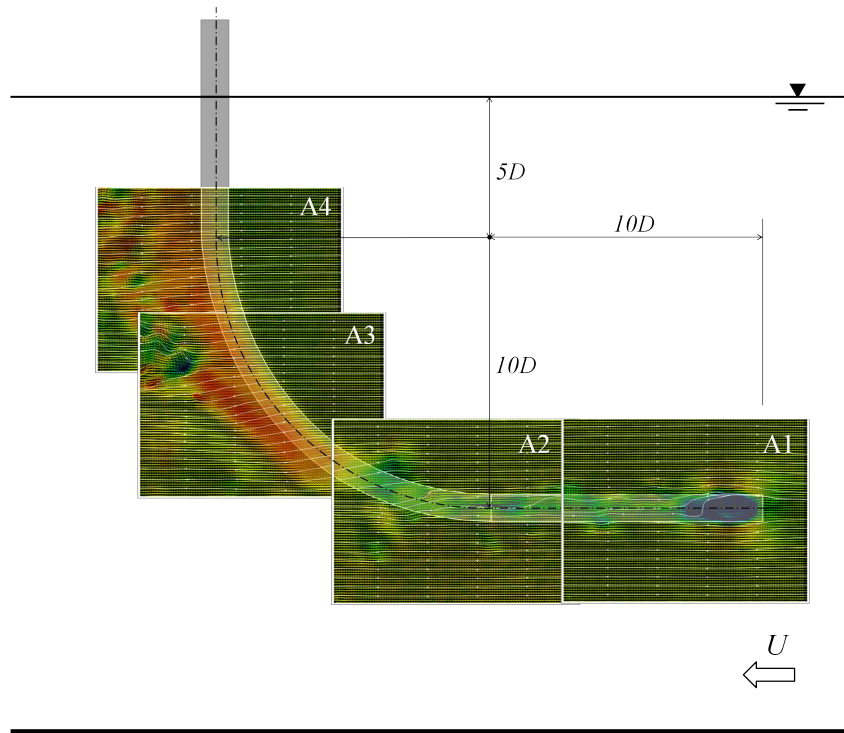


FIGURE 7: Composition of PIV velocity fields for concave configuration with $h/D = 5$.

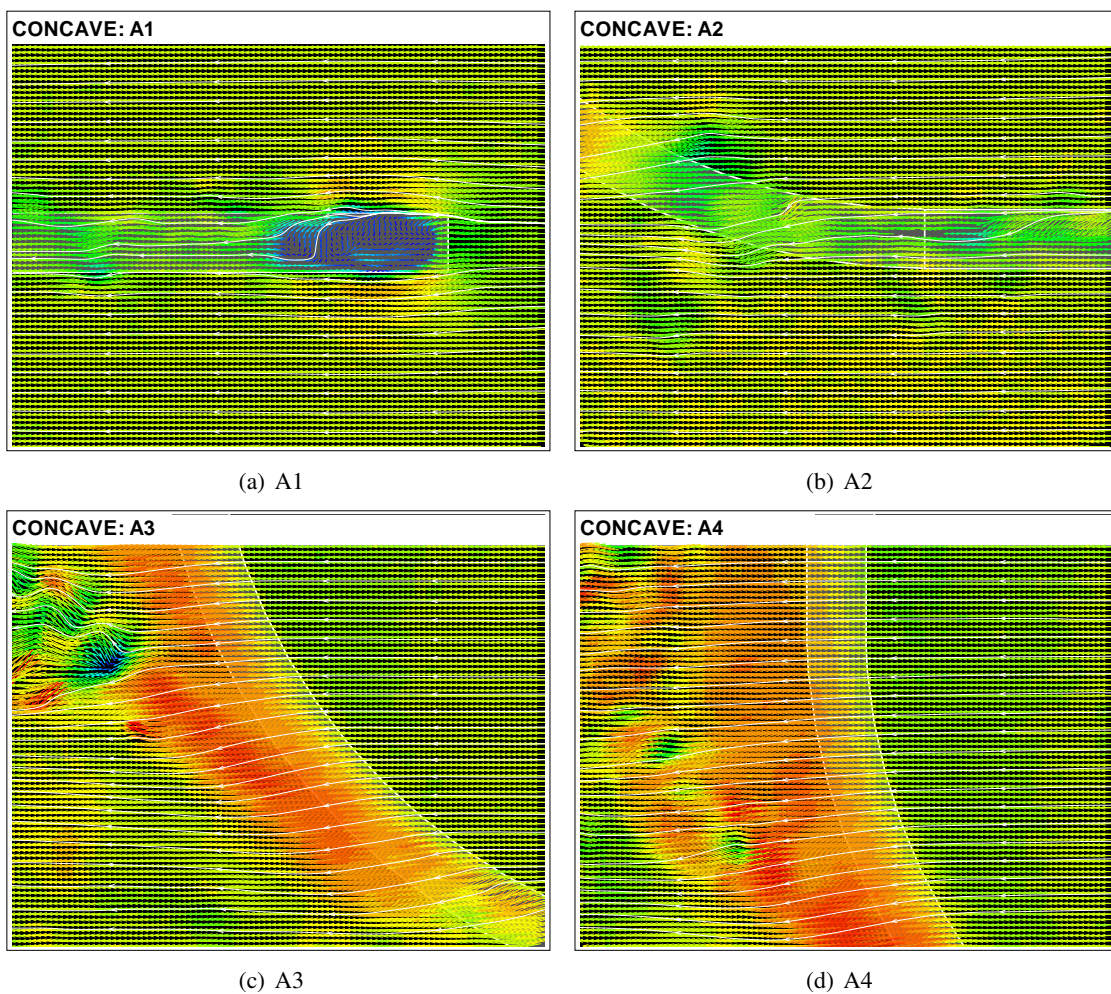


FIGURE 8: Detailed velocity fields from Figure 7. Flow direction is from right to left and vectors are coloured by velocity magnitude. $Re = 1000$.

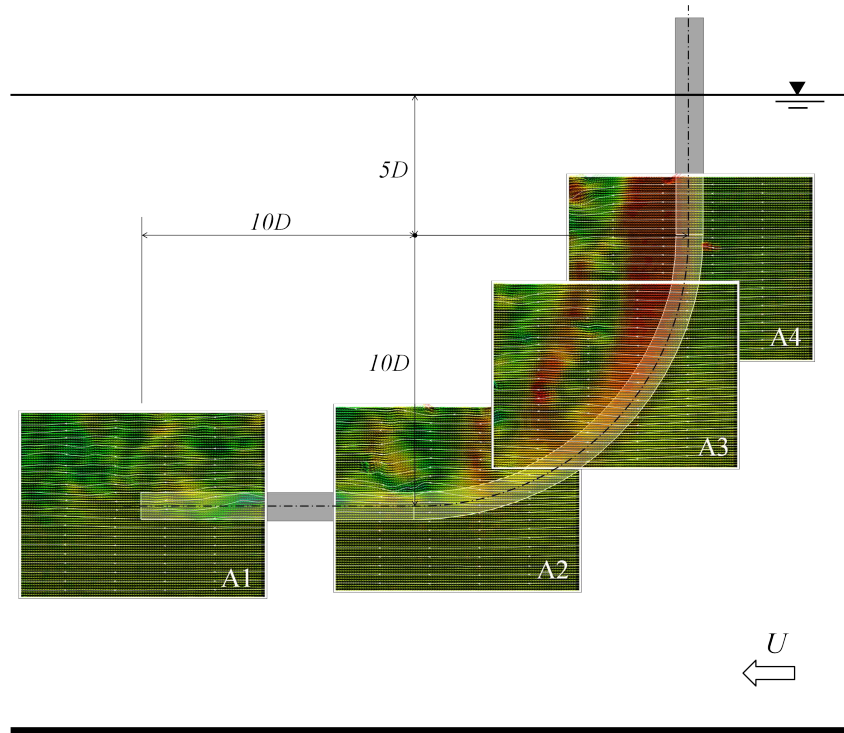


FIGURE 9: Composition of PIV velocity fields for convex configuration with $h/D = 5$.

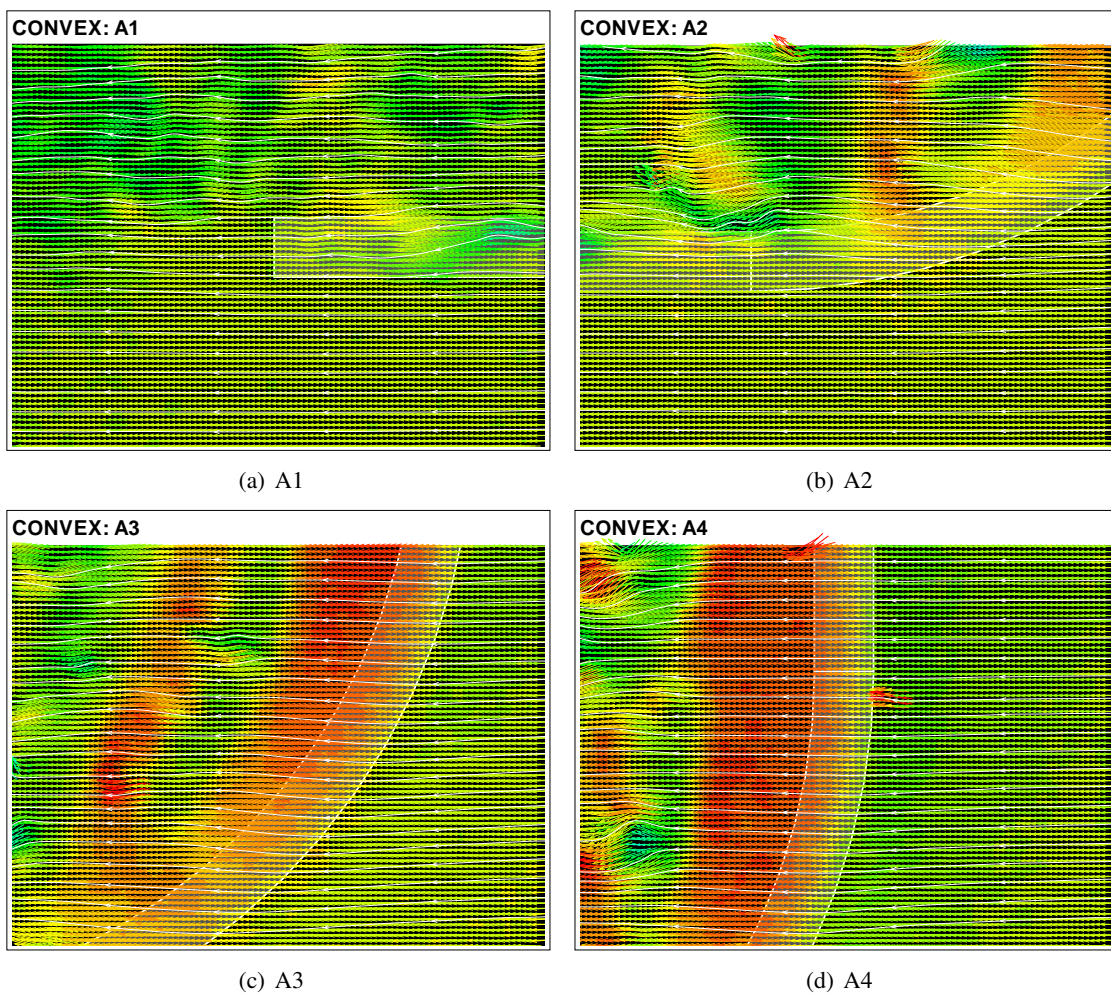


FIGURE 10: Detailed velocity fields from Figure 9. Flow direction is from right to left and vectors are coloured by velocity magnitude. $Re = 1000$.

the curvature in A3. This looks similar to Fig. 3 in Miliou et al. [3] for $Re = 100$.

THE EXCITATION MECHANISMS

The main question to be answered by the present study is concerned with the fact that the amplitude in the cross-flow direction for the convex configuration is able to drop down to 0.1 for high reduced velocities while the concave configuration sustains vibration around 0.35. We believe this distinct behaviour between the convex and the concave configurations is related to the wake interference happening in the lower half of the cylinder due to perturbations generated in the horizontal section when it is positioned upstream.

In the concave configuration the horizontal part of the cylinder is located upstream of the curved and vertical parts. The approaching flow encounters a circular blunt leading edge with a clear separation region around the circumference (Figure 8(a)). The flow that separates at the leading edge tends to create a separation bubble and latter reattach along the horizontal section of the cylinder. Because the cylinder already presents cross-flow and streamwise vibrations, the three-dimensional separation bubble will not find a stable configuration nor a definite reattachment region, instead it will develop a periodic behaviour that may result in three-dimensional vortices being shed downstream, reaching the other parts of the cylinder. This is very clear in areas A1 and A2 of Figures 7 and 8.

The fluid-elastic mechanism behind the response may be a composition of different phenomena acting at the same time. We believe this interaction between the disturbed flow from the upstream horizontal part with the curved and vertical parts is responsible for sustaining the level of vibration around $\hat{y}/D = 0.35$ and $\hat{x}/D = 0.35$. We suggest such an interaction may be occurring in the following forms:

(i) Vortices generated along the horizontal section may impinge on the curved part generating impulses in the same manner that large eddies of turbulence induce buffeting on elastic structures. Because the concave configuration has a longer section immersed in such a disturbed wake it is more susceptible to buffet. Evidence that a buffeting-like phenomenon might be occurring is that the streamwise vibration shows a considerable increase in amplitude with increasing flow speed further out of the synchronisation range. Figure 6(b) also reveals that these vibrations are not harmonic and may even be chaotic, another evidence supporting the buffeting-excitation hypothesis.

(ii) The disturbed flow from the horizontal part may

be disturbing and disrupting the vortex shedding mechanism from the curved and vertical sections, for example uncorrelating the vortex shedding mechanism in a curved region of the cylinder near the horizontal part. Also, the vortex wake along the curved-vertical half of the concave cylinder showed less correlation along the span, resulting in a lower peak of vibration during the synchronisation range.

(iii) Because the concave configuration has a fixed separation ring at the circle facing upstream, there might be some galloping-like instability related to the separation and reattachment of the three-dimensional bubble. This could generate non-resonant forces that could sustain some level of vibration for reduced velocities above the synchronisation range.

(iv) Finally, the concave configuration might experience some kind of instability related to the geometric arrangement of the experiment. Because the centre of pressure is located upstream of the vertical axis of the pendulum a minute deflection (or torsion) of the cylinder may result in a resolved force that will increase displacement. The opposite is true for the convex configuration in which the centre of pressure downstream of the vertical axis of the pendulum can only generate stabilising forces.

Of course all four mechanisms suggested above may also be occurring simultaneously or it may not even be possible to explain them separately. In addition, they might as well be very dependent on Reynolds number and amplitude of vibration.

CONCLUSIONS

We have investigated the VIV response of a curved cylinder in a concave and convex configurations regarding the approaching flow. We conclude that:

(i) In general terms, a curved cylinder presents a lower peak of amplitude of vibration in both the cross-flow and streamwise direction when compared to a straight cylinder. Nevertheless, a considerable level of streamwise vibration not attributed to VIV was observed for reduced velocity as high as 18.

(ii) Although the peak amplitude is reduced, a curved cylinder may present a significant level of vibration that is sustained for higher values of reduced velocity beyond the end of the typical synchronisation range.

(iii) The concave configuration shows a considerable level of cross-flow vibration around $\hat{y}/d = 0.35$ up to the highest reduced velocity performed in this experiment.

(iv) The overall response showed little dependency on the vertical length immediately below the water line, at least for a section varying between $h/D = 0$ and 10.

(v) We suggest that the flow-structure interaction mechanism that differentiates the concave from the convex response has its origin in the disturbed flow that separates from the horizontal part located upstream. This could be related to buffeting, galloping, disturbed VIV or geometric instabilities.

PIV measurements for an oscillating cylinder, especially at high reduced velocities, could throw some light into the actual mechanism of excitation.

ACKNOWLEDGEMENTS

G.R.S. Assi wishes to acknowledge the support of FAPESP (São Paulo State Research Foundation) through the research grant 2011/00205-6. N. Srinil is grateful to “The Sir David Anderson Award” from the University of Strathclyde.

REFERENCES

- [1] Assi, G.R.S., Bearman, P.W., Meneghini, J.R. **2010** On the wake-induced vibration of tandem circular cylinders: the vortex interaction excitation mechanism *J. Fluid Mech.*, 661, 365-401.
- [2] Srinil, N. **2010** Multi-Mode Interactions in Vortex-Induced Vibrations of Flexible Curved/Straight Structures with Geometric Nonlinearities *J. Fluids and Structures*, 26, 1098-1122.
- [3] Miliou, A., De Vecchi, A., Sherwin, S.J., Graham, M.R. **2007** Wake dynamics of external flow past a curved circular cylinder with the free stream aligned with the plane of curvature *J. Fluid Mech.*, 592, 89-115.
- [4] Assi, G.R.S., Meneghini, J.R., Aranha, J.A.P., Bearman, P.W., Casaprima, E. **2006** Experimental investigation of flow-induced vibration interference between two circular cylinders. *J. Fluids and Structures*, 22, 819-827.
- [5] Freire, C.M., Meneghini, J.R. **2010**. Experimental investigation of VIV on a circular cylinder mounted on an articulated elastic base with two degrees-of-freedom. *In the proceedings of BBVIV6 – IUTAM Symposium on Bluff Body Wakes and Vortex-Induced Vibrations*, 2010, Capri, Italy.
- [6] Assi, G.R.S., Bearman, P.W and Kitney, N **2009** Low Drag Solutions for Suppressing Vortex-Induced Vibration of Circular Cylinders. *J. Fluids and Structures* 25, 1-10.
- [7] Assi, G.R.S., Bearman, P.W., Kitney, N., Tognarelli, M.A. **2010** Suppression of Wake-Induced Vibration of Tandem Cylinders with Free-to-Rotate Control Plates. *J. Fluids and Structures*, 26, 1045-1057.
- [8] Freire, C.M., Korkischko, I., Meneghini, J.R. **2009** Development of an elastic base with tow degrees of freedom for VIV studies. *In the proceedings of COBEM 2009 – 20th International Congress of Mechanical Engineering*, 2009, Gramado, Brazil.
- [9] Freire, C.M., Korkischko, I., Meneghini, J.R. **2011** Defining a parameter of effectiveness for the suppression of vortex-induced vibration. *In the proceedings of OMAE2011 – 30th International Conference on Ocean, Offshore and Arctic Engineering*, 2011, Rotterdam, The Netherlands.